

CERN-TH-2023-229

disorder: Deep inelastic scattering at high orders

Alexander Karlberg

CERN, Theoretical Physics Department, CH-1211 Geneva 23, Switzerland

alexander.karlberg@cern.ch**Abstract**

We present a Fortran 77/95 code capable of computing QCD corrections in deep inelastic scattering (DIS). The code uses the Projection-to-Born method to combine an exclusive DIS + 1 jet calculation with the inclusive DIS structure functions, thereby obtaining fully differential DIS predictions at $\mathcal{O}(\alpha_s^2)$. The code is lightweight and fast, and yet includes the most common functionalities found in typical perturbative QCD programs, like automatic renormalisation and factorisation scale uncertainties, options to run and combine multiple seeds, and interfaces to `fastjet` and `LHAPDF`. Due to the underlying exclusive DIS + 1 jet code, the program also provides stable results in the infrared, relevant for extracting logarithmic coefficients for analytic resummations. As a by-product the code provides access to the DIS structure functions and (reduced) cross sections up to $\mathcal{O}(\alpha_s^3)$.

Contents

1	Introduction	2
2	Basics of the DIS process	3
2.1	A note on the phase space	5
2.2	Applying P2B	5
3	Running disorder	6
3.1	Compiling and prerequisites	6
3.1.1	The analysis framework	6
3.2	Inclusive mode	7
3.3	P2B mode	8
3.4	Validating the code	9
4	Benchmarks and results	9
4.1	Inclusive results	10
4.2	Exclusive laboratory frame results	10
5	Conclusion	11
	References	12

<https://github.com/alexanderkarlberg/disorder>

1 Introduction

Deep inelastic scattering (DIS) is arguably one of the best understood processes in perturbative QCD. It is one of few processes for which there exists an exact factorisation theorem [1, 2], and the massless unpolarised hard perturbative coefficients have been computed through an impressive three loops [3–15] with progress on the four loop results presented recently in Ref. [16]. Together with the three-loop results for the splitting functions [17, 18] and the four-loop β -function [19, 20] for the running coupling this allows for the determination of the proton structure functions at the next-to-next-to-next-to-leading order (N^3 LO).¹ The structure functions can be combined with an exclusive next-to-next-to-leading order (NNLO) DIS + 1 jet computation to obtain fully differential N^3 LO predictions in DIS, as was done by the NNLOJET collaboration [35, 36]. This computation uses the Projection-to-Born (P2B) method, which was first introduced in the context of NNLO Vector Boson Fusion (VBF) production [37].

Despite this impressive theoretical progress, there are few publically available computer codes from which one can obtain fast and reliable high-order differential cross section predictions for DIS. This paper and associated Fortran code seeks to address that.

One of the advantages of the P2B method is that it is rather agnostic towards the details of the underlying exclusive computation, and it is hence possible to “upgrade” existing fixed-order codes to one order higher. Historically the most successful fixed-order codes have been MEPJET [38], `disent` [39], `disaster++` [40], and `nlojet++` [41] which are all next-to-leading order (NLO) accurate. Discrepancies between `disent` and fixed-order coefficients from analytical resummation were initially observed in Refs. [42, 43], and were only recently understood to be due to a bug in one of the dipole terms for the gluon channel in `disent` [44, 45].

With the bug fixed we can use `disent` as the underlying exclusive NLO code together with the NNLO structure functions from HOPPET [46, 47].² Advantages of using `disent` are its well-known efficiency and numerical stability. The resulting program is dubbed `disorder` keeping in the spirit of previous names for fixed-order DIS codes.³ Since the program relies on HOPPET for the structure functions, the inclusive DIS cross section can actually be obtained one order higher, as the structure functions were implemented at N^3 LO already in the context of the `proVBFH` codes [37, 50–52] and are publically available since v1.3.0 of HOPPET [53].⁴ The `disorder` program therefore has two more or less separate use cases: 1. The computation of fully exclusive NNLO photon-mediated massless DIS 2. The computation of inclusive neutral-(NC) and charged-current (CC) massless DIS at N^3 LO accuracy.

The program is designed to be user-friendly with a simple command line interface. It prints cross sections and all important run-parameters to the screen and disk, allowing a user to acquire cross sections with very little effort. It comes with an interface to `fastjet` [54] and LHAPDF [55] and uses the histogramming package from the POWHEG-BOX [56] for easy analysis. The code can also compute renormalisation and factorisation scale uncertainties on-the-fly. For inclusive cross sections the code provides results in a matter of seconds⁵ even at N^3 LO with integration uncertainties typically below the permille level. For exclusive quantities

¹Technically the four-loop splitting functions are needed to claim this accuracy. Recent progress in determining those and the three-loop massive operator matrix elements can be found in Refs. [21–27] and [28–34] respectively. Phenomenologically the first few moments which have been computed therein, with some exact pieces also being known, are however in all likelihood enough to claim N^3 LO.

²The combination of `disent` and HOPPET naturally leads to a Fortran code. For a C++ alternative, based on publically available codes, one could have started from either `disaster++` or `nlojet++` and used the structure functions as implemented in APFEL++ [48, 49]

³`dispatch` [43] deserves an honorable mentioning in this context.

⁴HOPPET implements all known approximate and exact ingredients at this order - see footnote 1.

⁵The majority of this time is taken up by the structure function initialisation inside HOPPET rather than the integration of the cross section.

the code can be run on a laptop at NLO and depending on the analysis, and the laptop, even at NNLO.

It should be pointed out that the code provides little theoretical advance on its own. As described above, the structure functions themselves have been known for a little while, and the P2B method has already been applied to DIS, even one order higher than here.⁶ It is however the author's opinion that with the renewed interest in DIS due to the upcoming Electron-Ion-Collider (EIC) [60], well-maintained public code is extremely valuable for both the experimental and theoretical communities, and that providing documentation in the form of this article will enable the wide use of the code.

The paper is structured as follows: In section 2 we review the DIS process and kinematics as implemented in `disorder`. In section 3 we provide details on how to run `disorder` and in section 4 we show a few results from the program. Finally we conclude in section 5.

2 Basics of the DIS process

In this section we first give some standard definitions for kinematics and cross sections in DIS. Along the way we specify the conventions that are used in the `disorder` code, and provide some details on the P2B method as applied here.

At leading order (LO) the DIS process is the scattering of a massless (anti-)quark q off a massless (anti-)lepton l via the exchange of a photon or electroweak gauge boson V of virtuality Q^2 . Denoting the external four-momenta by k_i (incoming lepton), k_f (outgoing lepton), p_i (incoming quark), and p_f (outgoing quark) we can define the Lorentz invariant DIS variables x , Q^2 , and y , given by

$$Q^2 = -q^2 = -(k_i - k_f)^2, \quad x = \frac{Q^2}{2P \cdot q}, \quad y = \frac{P \cdot q}{P \cdot k_i} = \frac{p_i \cdot q}{p_i \cdot k_i}, \quad (1)$$

where P is the hadron four-momentum. As can be seen these kinematics are fully specified by the hadron and lepton momenta. This is also true beyond LO. DIS is most often analysed in the Breit-frame which is specified⁷ by requiring that $2x\vec{P} + \vec{q} = 0$. In this frame the mediated vector boson has zero energy component and is anti-aligned with the incoming parton. Explicitly in `disorder` the Breit-frame at LO is

$$k_i = \frac{Q}{2} \left(\frac{2-y}{y}, \frac{2\sqrt{1-y}}{y}, 0, -1 \right), \quad p_i = \frac{Q}{2} (1, 0, 0, +1) \quad (2)$$

$$k_f = \frac{Q}{2} \left(\frac{2-y}{y}, \frac{2\sqrt{1-y}}{y}, 0, +1 \right), \quad p_f = \frac{Q}{2} (1, 0, 0, -1)$$

where four-momenta are given as (E, p_x, p_y, p_z) . The resulting vector q is hence given by $(0, 0, 0, -Q)$. In the laboratory frame we align the parton with the positive z -axis and hence the lepton with the negative

$$\tilde{k}_i = E_l (1, 0, 0, -1), \quad \tilde{p}_i = x E_h (1, 0, 0, +1) \quad (3)$$

where E_h is the energy of the incoming hadron. Using the definitions of eq. (1) one finds that in the lab frame

$$\tilde{q} = (y(E_l - x E_h), -Q\sqrt{1-y}, 0, -y(E_l - x E_h)) \quad (4)$$

⁶It has also been applied in polarised DIS in Refs. [44, 45, 57–59].

⁷For the explicit transformation between lab- and Breit-frames we follow Appendix 7.11 in Ref. [61].

and the outgoing momenta then simply follow from momentum conservation

$$\tilde{k}_f = \tilde{k}_i - \tilde{q}, \quad \tilde{p}_f = \tilde{p}_i + \tilde{q}. \quad (5)$$

The inclusive cross section for DIS can be split into a NC contribution, from $e^\pm p \rightarrow e^\pm + X$ scattering, and a CC contribution from $e^\pm p \rightarrow \nu + X$ ⁸ scattering. The unpolarised NC cross section can be written as

$$\frac{d\sigma_{\text{NC}}^\pm}{dx dQ^2} = \frac{2\pi\alpha^2}{xQ^4} [y_+ F_2^{\text{NC}} \mp y_- x F_3^{\text{NC}} - y^2 F_L^{\text{NC}}], \quad (6)$$

where $y_\pm = 1 \pm (1-y)^2$, α is the fine structure constant and F_i^{NC} can be expressed in terms of the usual proton structure functions

$$\begin{aligned} F_i^{\text{NC}} &= F_i^\gamma - v_e \Gamma_{\gamma Z} F_i^{\gamma Z} + (v_e^2 + a_e^2) \Gamma_Z F_i^Z, \quad i = 2, L \\ F_3^{\text{NC}} &= -a_e \Gamma_{\gamma Z} F_3^{\gamma Z} + 2v_e a_e \Gamma_Z F_3^Z. \end{aligned} \quad (7)$$

Here $v_e = -\frac{1}{2} + 2 \sin^2 \theta_W$ is the vector and $a_e = \frac{1}{2}$ is the axial-vector coupling, M_Z is the Z boson mass, $\Gamma_{\gamma Z} = \frac{Q^2}{\sin^2 2\theta_W (Q^2 + M_Z^2)}$, and $\Gamma_Z = \Gamma_{\gamma Z}^2$. θ_W is the weak mixing angle. In disorder the electroweak parameters are fixed by α , M_W , and M_Z through the tree-level relations

$$\sin^2 \theta_W = 1 - \frac{M_W^2}{M_Z^2}, \quad G_F = \frac{\pi\alpha}{\sqrt{2}m_W^2 \sin^2 \theta_W}, \quad (8)$$

with G_F the Fermi constant. Similarly we define the unpolarised CC cross section as

$$\frac{d\sigma_{\text{CC}}^\pm}{dx dQ^2} = \frac{\pi\alpha^2}{8 \sin^4 \theta_W x} \left[\frac{1}{M_W^2 + Q^2} \right]^2 [y_+ F_2^{\text{CC}} \mp y_- x F_3^{\text{CC}} - y^2 F_L^{\text{CC}}], \quad (9)$$

where M_W is the mass of W boson and the CC structure functions are now simply given by the W ones

$$F_2^{\text{CC}} = F_2^{W^\pm}, \quad F_L^{\text{CC}} = F_L^{W^\pm}, \quad F_3^{\text{CC}} = F_3^{W^\pm}. \quad (10)$$

The exact definitions of all proton structure functions inside HOPPET up to N³LO can be found in Refs. [46, 47, 53]. The tabulation of the structure functions inside HOPPET, as used in disorder, has a relative numerical precision of 10^{-4} for most values of x , which in turn limits the accuracy which can be obtained to the same order.

In DIS it is also customary to define the dimensionless *reduced* NC and CC cross sections by [62]

$$\begin{aligned} \tilde{\sigma}_{\text{NC}}^\pm(x, Q^2) &= \frac{xQ^4}{2\pi\alpha^2} \frac{1}{y_+} \frac{d\sigma_{\text{NC}}^\pm}{dx dQ^2} \\ \tilde{\sigma}_{\text{CC}}^\pm(x, Q^2) &= \frac{8 \sin^4 \theta_W x}{\pi\alpha^2} [M_W^2 + Q^2]^2 \frac{d\sigma_{\text{CC}}^\pm}{dx dQ^2}. \end{aligned} \quad (11)$$

disorder provides direct access to all the cross sections in eqs. (6), (9), and (11) at N³LO accuracy. In principle one can also access the NC and CC structure functions, although they are currently only computed as an intermediate step to construct the cross sections and are not accessible in the user analysis.

⁸Here $\nu = \{\nu_e, \bar{\nu}_e\}$ for e^- and e^+ respectively. One can of course also consider incoming neutrinos which does not change the discussion here.

2.1 A note on the phase space

Since the Born phase space is fully constrained by specifying any two of the three DIS variables x , y , and Q^2 there exists more than one double-differential cross section. The convention in `disorder` is to always return $\frac{d\sigma^2}{dx dQ^2}$ (in pb/GeV²) regardless of which of the two variables are fixed. The user can easily convert to $\frac{d\sigma^2}{dx dy}$ or $\frac{d\sigma^2}{dy dQ^2}$ by supplying a factor $\frac{Q^2}{y}$ or $\frac{x}{y}$ respectively. If only one of x , y , or Q^2 is specified then the appropriate single differential cross section is returned, i.e. $\frac{d\sigma}{dx}$ in pb, $\frac{d\sigma}{dy}$ in pb, or $\frac{d\sigma}{dQ^2}$ in pb/GeV², integrated over the other two variables. If none of the variables are fixed then the total cross section integrated over x , y , and Q^2 is returned in pb.

2.2 Applying P2B

The structure functions are by definition inclusive in all radiation and can therefore only provide predictions for quantities, like the inclusive cross sections, which depend on the Born kinematics of eq. (1) only. If we instead evaluate the structure functions on an observable sensitive to emissions, e.g. the transverse momentum of the hardest jet in the laboratory frame, we see that this will not give the right answer, as the real emissions are not included with their correct kinematics.

The P2B method lifts this restriction by effectively replacing the Born-kinematics real-emission contributions in the structure functions with the correct kinematics ones. In practice whenever `disent` returns an event with some weight, we bin it once according to the true kinematics, and again projecting the kinematics to the underlying Born changing the sign of the weight. This last term, upon integration, will exactly cancel the real contribution in the structure functions, whereas the first term will provide the correct real matrix element.

The projections themselves are trivial because, as outlined above, the Born kinematics are fully specified at all orders by the lepton (and proton) momenta, as given in eqs. (2)–(5). Hence computing the projections adds very little computational effort to the cross section calculation.

At this point it is worth reminding the reader that `disent` only includes the photon-mediated NC, and hence `disorder` only provides exclusive predictions for this channel. It should in principle be possible to extend the code to include Z-mediation (including interferences) and CC, but we leave this for future work.

In principle P2B could be applied to the `disent` code without any major modifications besides the bug fix mentioned in the introduction. However a few significant modifications were introduced to allow for a more flexible integration of `disent` into `disorder`. The version of `disent` that we include in `disorder` is based on the version which can be found in `dispatch` [43], and which already included some minor modifications. In addition to the modifications present there, we have also introduced α as an input parameter, whereas before it was fixed to 1/137. A number of parameters can also now be set on the command line as described below. Besides coding the actual interface to `disent`, the biggest modification introduced in `disorder` is that the `KPFUNS` subroutine now returns an array of weights corresponding to varying the factorisation scale by a factor two up and down. This allows for much faster evaluation of scale uncertainties compared to running the program three separate times. Additionally `disent` can now also use any scale defined in terms of x , y , and Q , and not just some multiple of Q . We provide a few different scale choices as documented below, but more can easily be implemented.

3 Running disorder

In this section we give instructions on how to compile and run `disorder`, giving a few examples of the use of the most common command line arguments. The code itself can be obtained from

<https://github.com/alexanderkarlberg/disorder>

3.1 Compiling and prerequisites

A user should start by inspecting [README.md](#). To compile `disorder` both `HOPPET` (v1.3.0 or later) and `LHAPDF` (tested with v6.5.4) [55] have to be installed on the machine. If both are installed in a location in the `$PATH` it is enough to run

```
mkdir build && cd build
cmake ..

make [-j]
```

from the main directory. This will create an executable `disorder` along with two auxiliary executables, `mergedata` and `getpdfuncert`. For non-standard installation of `HOPPET` and `LHAPDF` the paths can be specified like this

```
cmake -DHOPPET_CONFIG=/path/to/hoppet-config -DLHAPDF_CONFIG=/path/to/lhapdf-config
```

where the path should include the config-file itself (i.e. `/usr/local/bin/hoppet-config`). By default `fastjet` is not linked and only a skeleton analysis ([analysis/simple_analysis.f](#)) is compiled. To link `fastjet` run

```
cmake -DNEEDS_FASTJET=ON [-DFASTJET_CONFIG=/path/to/fastjet-config]
```

where the path to `fastjet-config` only needs to be specified if it is not in the user's `$PATH`. To compile a different analysis the user should first put it in the [analysis](#) directory (here we assume it to be called `my_analysis.f`), and then pass it to `cmake` through

```
cmake -DANALYSIS=my_analysis.f
```

The program has been found to compile on a Linux machine using the `gfortran v11.4.0` compiler and also on various MacOS systems.

3.1.1 The analysis framework

The code uses the `POWHEG-BOX` analysis framework, with some minor modifications. A few example analyses are included in the `analysis` directory. Any new analysis should be put here and the name of the analysis should be passed to `cmake` as described above. There are two mandatory routines in the analysis file, `define_histograms` and `user_analysis`. In the first routine one should define histograms like this (there are also routines available to book histograms with varying bins sizes)

```
call bookupeqbins('string_name', binsize, min, max)
```

The `user_analysis` routine takes as input

```
integer n
double precision dsig(maxscales), x, y, Q2
```

where `n` is the number of initial plus final state particles, `dsig` is the weights computed by `disorder` and `maxscales` is the maximum number of scales which is supported (currently 7). `x`, `y`, and `Q2` are the DIS variables.

Through the module `mod_analysis` the analysis has access to two array of momenta `pbreit(0:3,1:n)` and `plab(0:3,1:n)` in which the Breit and laboratory frame momenta are stored respectively. The first entry is the incoming lepton, the second the incoming parton, the third the outgoing lepton and the rest outgoing partons. The output of the analysis will be saved to the disk as outlined below. In the `user_analysis` routine the user should perform their analysis and fill histograms like this

```
call filld('string_name', obs_value, dsig)
```

where `obs_value` is the value of the observable to be binned, and `dsig` is the associated array of weights.

In the `aux` folder one may also find a script called `mergedata` that can perform various manipulations of the datafiles. In particular

```
./mergedata 1 {list of statistically equivalent files}
```

will take the average of all files and produce the file `fort.12` with the result. Running the script without any arguments will result in a list of possible uses of the script. The `mergedata` script is taken from the POWHEG-BOX as well.

3.2 Inclusive mode

The syntax for running the program is

```
./disorder -pdf LHAPDF_name [options]
```

Running the program without any other options than `-pdf` will compute the total inclusive cross section above the minimum Q value accessible in the PDF, and using default parameters everywhere. The user can get a list of most parameters which can be specified on the command line by running

```
./disorder -help
```

Here we describe the most common flags, but for a complete list of all parameters, and their use, the user should look through the file `src/mod_parameters.f90`.

The program allows the user to specify limits on x , y , and Q through `-xmin`, `-xmax`, `-ymin`, `-ymax`, `-Qmin`, `-Qmax`, or to fix them through the options `-x`, `-y`, `-Q`. For instance to compute the cross section at $Q = 20$ GeV and $x > 0.01$ one would run

```
./disorder -Q 20 -xmin 0.01 -pdf LHAPDF_name
```

The program will perform a Monte Carlo integration in the ranges specified, using the integrator VEGAS [63]. If the phase space is fully constrained by fixing two of either x , y , and Q the program simply evaluates one point and returns the answer.

One can further specify the energy of the incoming lepton through `-Elep`, the incoming hadron through `-Ehad`. By default the lepton is taken to be an electron but specifying `-positron` on the command line will change that. The code computes the photon-mediated NC cross section only by default. To include the Z one can specify `-includeZ` and to include CC processes one can specify `-CC`. The inclusion of NC processes can also be controlled through the `-NC` flag. In fact, all logical flags can be prefixed by “no” to turn them off. Hence the below command line would run the program with CC processes only using a positron

```
./disorder -Q 20 -xmin 0.01 -noNC -CC -positron -pdf LHAPDF_name
```

The order of the calculation is by default NNLO but can be specified with one of the flags `-lo/-nlo/-nnlo/-n3lo`. If the user wants to compute PDF uncertainties, the flag `-pdfuncert` should be given. This flag will make `disorder` loop over all the members in the PDF, and combine their errors according to the routine `getpdfuncertainty` [64], native to LHAPDF. This also means that the program is slowed down proportionally to the number of

PDF members (although the VEGAS grid only gets computed once and then stored so that the runs are fully correlated). If the PDF also includes α_s variations these are included in the PDF uncertainty by default. If the user wants the PDF and α_s uncertainties independently, then the flag `-alphasuncert` should be specified. Some care should be taken here, as in practice the code assumes that the α_s variations are contained in the last two PDF members, and simply separates them from the rest.

Renormalisation, μ_R , and factorisation, μ_F , scale uncertainties can be included by specifying the flag `-scaleuncert`. `disorder` uses the vector boson virtuality, Q^2 , as its default central scale, but can use any scale as long as it is defined in terms of x , y , and Q . A few central scales, μ , are currently implemented and can be accessed through the `-scale-choice` flag. The options are 1 (default): Q^2 , 2: $Q^2(1-y)$, 3: $\frac{Q^2(1-x)}{x}$. The program will then compute a standard 7-point scale variation varying this scale by a factor of two up and down keeping $1/2 \leq \mu_R/\mu_F \leq 2$. On the screen the envelope of all 7 runs will be printed. The user can in principle also carry out arbitrary variations in individual runs by specifying `-xmur` and `-xmuf` on the command line. Here `xmur` is the ratio of μ_R/μ and similarly for `xmuf`.⁹

Finally the random seed can be set with the `iseed` flag. When the program terminates it will print results to screen but also save a number of files depending on the exact input. There is always a file called `xsct_nnlo_seed0001.dat`, where the `nnlo` and `seed0001` parts will vary depending on the order and seed, which contains a summary of the run, including the total and reduced cross sections.

The output of the analysis is printed to a number of `.dat` files, the number depending on the input, prefixed by `disorder_nnlo_seed0001_pdfmem000` where again the exact prefix will depend on the input. The output name also contains information on the seed, the PDF member and the renormalisation and factorisation scales if `-scaleuncert` is on. The user can specify a prefix to be added to all the files through the `-prefix` flag.

Since it is often not necessary to run an analysis in the inclusive mode, the user can simply turn this off with the `-no-analysis` flag.

Finally the user can control the number of VEGAS integration points through the two flags `-ncall1` and `-ncall2`. The first flag controls the number of points to use to set up the grids. Since the phase space is not complicated it is rarely necessary to increase the default of 10000. The second flag controls the number of points that are used for the actual integration. If one is not running an analysis, the default number of 100000 should give results that have better than permille level accuracy. If the user wishes for instance to bin the cross section in fine bins of x and Q^2 , this number will most likely have to be increased.

3.3 P2B mode

To turn on P2B it is enough to specify `-p2b` on the command line. Many of the flags described above can also be specified in this mode, with a few limitations

- `-CC` and `-includeZ` are not supported
- `-n3lo` is not supported
- `-pdfuncert` and `-alphasuncert` are not supported

Importantly, it is possible to run with the `-scaleuncert` flag which leads to a significant reduction in run-time compared to doing seven separate runs. When running in P2B mode it

⁹In practice it is faster to use the `-scaleuncert` flag as the program will only recompute what is needed for the variations rather than do a full event. However, at N³LO, in general, this is not true, due to the fact that the number of tables needed in HOPPET to carry out on-the-fly scale variations increases dramatically at this order, compared to using a fixed ratio of Q . Given how fast the code is, it is still the author's opinion that it is more convenient to use the on-the-fly variations.

$$Q = 10 \text{ GeV}, \quad x = 0.01$$

	$\frac{\sigma_{\text{NC}}}{dx dQ^2} [\text{pb/GeV}^2]$	δPDF	$\frac{\sigma_{\text{CC}}}{dx dQ^2} [\text{pb/GeV}^2]$	δPDF	$\tilde{\sigma}_{\text{NC}}$	$\tilde{\sigma}_{\text{CC}}$
aN ³ LO	$1932^{+705\%}_{-486\%}$	0.972%	$1.100^{+591\%}_{-423\%}$	1.103%	0.8174	2.884
N ³ LO	$1886^{+546\%}_{-160\%}$	0.845%	$1.080^{+455\%}_{-132\%}$	0.914%	0.7980	2.829
NNLO	$1895^{+150\%}_{-118\%}$	0.840%	$1.084^{+125\%}_{-994\%}$	0.908%	0.8018	2.840
NLO	$1952^{+366\%}_{-443\%}$	0.810%	$1.111^{+302\%}_{-363\%}$	0.880%	0.8260	2.913
LO	$2058^{+13.8\%}_{-17.0\%}$	0.843%	$1.163^{+11.4\%}_{-14.1\%}$	0.885%	0.9708	3.050

Table 1: The inclusive and reduced cross sections at various orders in both NC and CC DIS. The setup is given in eq. (12). The aN³LO row is obtained using the approximate N³LO PDF set MSHT20an3lo_as118. Note that there is no Monte Carlo error on these numbers.

is furthermore of use to be able to control the number of calls to `disent`. This is done through the flag `-ncall2`, introduced already above.

We provide a small script to run on multiple cores on a single machine in [aux/runpar.sh](#).

3.4 Validating the code

The code comes with a script to validate that the results come out as expected. It can be run by entering `validation` and executing

```
./validate_or_generate.sh validate
```

The script builds the code and executes a number of tests designed to check the most important features of `disorder`, including both the NC and CC channels, the `fastjet` and `LHAPDF` interfaces, the automated PDF and scale uncertainty features, and `P2B`. The script assumes default installation paths for `HOPPET`, `fastjet`, and `LHAPDF`. A user can however manually change this by inspecting the script and adding the appropriate `cmake` flags at the beginning. The validation script runs in about 500 CPU seconds, or no more than a few minutes on a modern laptop.

4 Benchmarks and results

In this section we show a few results obtained by running the code in both the inclusive and the `P2B` modes. The purpose is not to provide an exhaustive phenomenological analysis, but rather show the capabilities of `disorder` and to provide a few select results that can be used to either validate the code when running it, or to validate other programs in the future. All analyses used in this section can be found in the [analysis](#) directory, and the raw results can be found in the [paper_runs](#) folder.

We use `fastjet v3.4.1` for jet-clustering, and unless otherwise stated we collide electrons and protons using the `MSHT20nnlo_as118 [65]` PDF set using `LHAPDF v6.5.4` and the following input parameters in all calculations

$$M_W = 80.398 \text{ GeV}, \quad M_Z = 91.1876 \text{ GeV}, \quad E_h = 920 \text{ GeV}, \quad E_l = 27.6 \text{ GeV}, \quad (12)$$

$$\alpha = 1/137, \quad \alpha_s(M_Z) = 0.118, \quad n_f = 5.$$

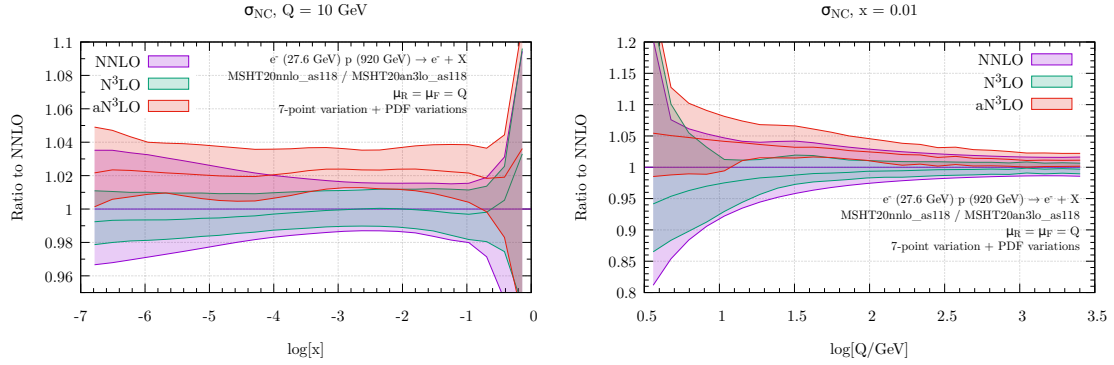


Figure 1: The NC cross section for fixed $Q = 10$ GeV differential in $\log x$ (left) and for fixed $x = 0.01$ and differential in $\log Q$ (right). We show NNLO (purple), N^3 LO (green), and aN^3 LO (red). The uncertainty band is obtained as the linear combination of scale and PDF uncertainties.

4.1 Inclusive results

The perhaps most fundamental question one can ask in DIS is “what is the total cross section for a given value of x and Q ?”. The answer to that question is given in table 1 for both the NC and CC channels at $Q = 10$ GeV and $x = 0.01$, at all available perturbative orders. The row aN^3 LO is obtained with the MSHT20an3lo_as118 [66] PDF set which includes approximate N^3 LO theoretical input. It is interesting to note that the inclusion of the approximate terms has an impact that is parametrically of the same order as the NNLO corrections. The PDF uncertainties stay more or less constant across all orders, which is not unexpected given that we use the same PDF at each order. To give a sense of the speed of the code, the combined results presented in the table, which corresponds to 325 different PDF members and hence structure functions, took a total of 3.5 minutes to obtain on a laptop equipped with an Intel i9-10885H CPU.

In figure 1 we show the NC cross section for fixed $Q = 10$ GeV (left) or $x = 0.01$ (right), now only at NNLO, N^3 LO and aN^3 LO. The uncertainty bands are obtained as a linear combination of the scale uncertainty and the PDF uncertainty, and is typically dominated by the latter, in particular at N^3 LO. We observe that although the central prediction at aN^3 LO is in tension with the N^3 LO curve, it is contained within the NNLO scale uncertainty band, except at intermediate x values. It will be interesting to see, if the inclusion of the exact N^3 LO splitting functions, when they become available, will ameliorate this tension.

4.2 Exclusive laboratory frame results

To demonstrate the results of the code in P2B mode, we perform a jet analysis in laboratory frame, based on Ref. [59], which probes the kinematic range accessible by the upcoming EIC. For this analysis we set $E_l = 18$ GeV, $E_h = 275$ GeV, and restrict the DIS kinematics by

$$25 \text{ GeV}^2 < Q^2 < 1000 \text{ GeV}^2, \quad 0.04 < y < 0.95. \quad (13)$$

We reconstruct jets in the laboratory frame using the anti- k_T algorithm [67] with $R = 0.8$. Jets are those that satisfy the following transverse momentum and pseudo-rapidity requirements

$$p_{t,j} > 5 \text{ GeV}, \quad |\eta_j| < 3. \quad (14)$$

In Fig. 2 we show the inclusive jet transverse momentum and rapidity at LO, NLO, and NNLO,

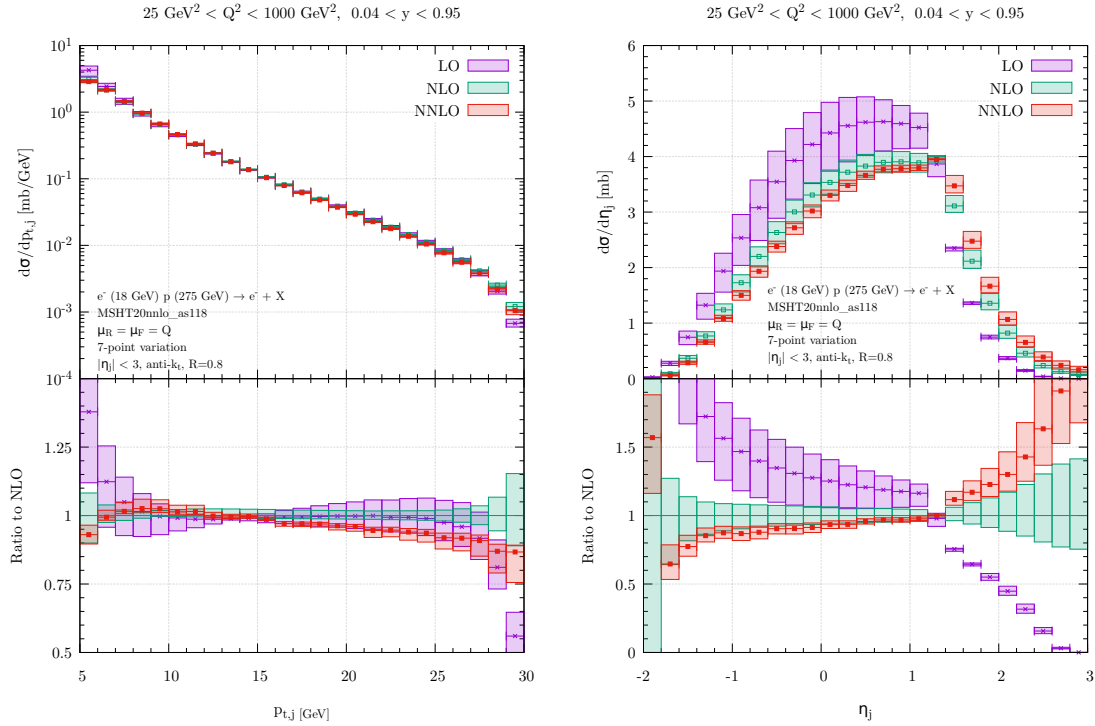


Figure 2: The NC cross section for fixed $Q = 10$ GeV differential in $\log x$ (left) and for fixed $x = 0.01$ and differential in $\log Q$ (right). We show NNLO (purple), N^3 LO (green), and aN^3 LO (red). The uncertainty band is obtained as the linear combination of scale and PDF uncertainties.

in photon-induced NC DIS. For the transverse momentum the higher order corrections are moderate except for small values and close to the LO threshold of $p_{t,j} = Q$. The rapidity distribution on the other hand receives larger corrections. This is in part due to hard jets with $p_{t,j} > Q$ that can only arise at NLO and beyond. Here the scale variation bands do not cover the actual corrections, and it is obvious that one needs to go beyond NLO for reliable predictions. Of course one needs the full N^3 LO to assess the reliability of the NNLO result. However, from similar results in Ref. [35] it can be expected that the actual N^3 LO results will be mostly contained within the scale variation band at NNLO.

5 Conclusion

In this paper we have presented version 1.0.0 of a Fortran code, `disorder`, capable of computing massless DIS cross sections fully differentially at NNLO and inclusively at N^3 LO. The code combines the structure functions from `HOPPET` and the exclusive DIS + 1 jet calculation of `disent`, using the P2B method. In the inclusive mode the program includes all NC and CC contributions and can carry out both scale and PDF variations on the fly. Due to the underlying tabulation of the structure functions in `HOPPET`, the code is extremely fast, and a user can obtain cross section results at N^3 LO in a matter of seconds.

In the fully differential P2B mode, only photon-mediated DIS can be computed, and no PDF variations are currently implemented. It should in principle be possible to extend `disent` to full NC and CC, and this is something that is planned for a future release of the code. Similarly the PDF variations could also be implemented, however this would require some

serious restructuring of the code for it to be efficient. Extension of the code to handle incoming neutrino beams, of relevance to the FASER [68] physics program, is also planned.

The upgrade of the code to handle $N^3\text{LO}$ fully differentially is however not currently planned. This is mainly due to the fact that this would require a complete replacement of `disent` with a proper exclusive NNLO DIS + 1 jet code, entailing a significant amount of work. Such a code would also be very slow compared to what is in place now, and it would defeat part of the attraction of `disorder` which is its speed. At LO and NLO a user can obtain differential results on a laptop running for a just a few minutes, and even reasonable NNLO results can be obtained on a multi-core machine running for an hour. $N^3\text{LO}$ results would inevitably require large resources on a High Performance Cluster.

Given the code's dependency on HOPPET, any developments therein will almost automatically propagate to `disorder`. In particular it is expected that the exact $\mathcal{O}(\alpha_s^4)$ splitting functions, as opposed to the approximations which are currently employed, will become available in HOPPET once they have been fully determined. This is currently the only missing piece needed to formally claim full $N^3\text{LO}$ accuracy for the structure functions. Similarly, were the massive DIS coefficient functions [69–76] to be implemented in HOPPET the structure functions in `disorder` could immediately be modified to accommodate this.

The code is intended to be user-friendly and to this effect comes with an interface to `fastjet` and LHAPDF and is run through a command line interface.

Acknowledgements

The author is grateful for many discussions with Andrea Banfi and Gavin Salam regarding `disent`, and for encouragement to publish `disorder`. The author also thanks Valerio Bertone for discussions about the DIS structure functions and Alex Huss for valuable cross-checks against results obtained with the NNLOJET code. The idea for the code originated while the author was working on Ref. [77].

References

- [1] J. C. Collins and D. E. Soper, *The Theorems of Perturbative QCD*, Ann. Rev. Nucl. Part. Sci. **37**, 383 (1987), doi:[10.1146/annurev.ns.37.120187.002123](https://doi.org/10.1146/annurev.ns.37.120187.002123).
- [2] J. C. Collins, D. E. Soper and G. F. Sterman, *Factorization of Hard Processes in QCD*, Adv. Ser. Direct. High Energy Phys. **5**, 1 (1989), doi:[10.1142/9789814503266_0001](https://doi.org/10.1142/9789814503266_0001), [hep-ph/0409313](https://arxiv.org/abs/hep-ph/0409313).
- [3] J. Sanchez Guillen, J. Miramontes, M. Miramontes, G. Parente and O. A. Sampayo, *Next-to-leading order analysis of the deep inelastic $R = \sigma_L / \sigma_{\text{total}}$* , Nucl. Phys. B **353**, 337 (1991), doi:[10.1016/0550-3213\(91\)90340-4](https://doi.org/10.1016/0550-3213(91)90340-4).
- [4] W. L. van Neerven and E. B. Zijlstra, *Order α_s^{**2} contributions to the deep inelastic Wilson coefficient*, Phys. Lett. B **272**, 127 (1991), doi:[10.1016/0370-2693\(91\)91024-P](https://doi.org/10.1016/0370-2693(91)91024-P).
- [5] E. B. Zijlstra and W. L. van Neerven, *Order α_s^{**2} QCD corrections to the deep inelastic proton structure functions F_2 and $F(L)$* , Nucl. Phys. B **383**, 525 (1992), doi:[10.1016/0550-3213\(92\)90087-R](https://doi.org/10.1016/0550-3213(92)90087-R).

- [6] E. B. Zijlstra and W. L. van Neerven, *Order α_s^2 correction to the structure function $F_3(x, Q^2)$ in deep inelastic neutrino - hadron scattering*, Phys. Lett. B **297**, 377 (1992), doi:[10.1016/0370-2693\(92\)91277-G](https://doi.org/10.1016/0370-2693(92)91277-G).
- [7] W. L. van Neerven and A. Vogt, *NNLO evolution of deep inelastic structure functions: The Nonsinglet case*, Nucl. Phys. B **568**, 263 (2000), doi:[10.1016/S0550-3213\(99\)00668-9](https://doi.org/10.1016/S0550-3213(99)00668-9), [hep-ph/9907472](https://arxiv.org/abs/hep-ph/9907472).
- [8] W. L. van Neerven and A. Vogt, *NNLO evolution of deep inelastic structure functions: The Singlet case*, Nucl. Phys. B **588**, 345 (2000), doi:[10.1016/S0550-3213\(00\)00480-6](https://doi.org/10.1016/S0550-3213(00)00480-6), [hep-ph/0006154](https://arxiv.org/abs/hep-ph/0006154).
- [9] S. Moch and J. A. M. Vermaseren, *Deep inelastic structure functions at two loops*, Nucl. Phys. B **573**, 853 (2000), doi:[10.1016/S0550-3213\(00\)00045-6](https://doi.org/10.1016/S0550-3213(00)00045-6), [hep-ph/9912355](https://arxiv.org/abs/hep-ph/9912355).
- [10] S. Moch, J. A. M. Vermaseren and A. Vogt, *The Longitudinal structure function at the third order*, Phys. Lett. B **606**, 123 (2005), doi:[10.1016/j.physletb.2004.11.063](https://doi.org/10.1016/j.physletb.2004.11.063), [hep-ph/0411112](https://arxiv.org/abs/hep-ph/0411112).
- [11] J. A. M. Vermaseren, A. Vogt and S. Moch, *The Third-order QCD corrections to deep-inelastic scattering by photon exchange*, Nucl. Phys. B **724**, 3 (2005), doi:[10.1016/j.nuclphysb.2005.06.020](https://doi.org/10.1016/j.nuclphysb.2005.06.020), [hep-ph/0504242](https://arxiv.org/abs/hep-ph/0504242).
- [12] A. Vogt, S. Moch and J. Vermaseren, *Third-order QCD results on form factors and coefficient functions*, Nucl. Phys. B Proc. Suppl. **160**, 44 (2006), doi:[10.1016/j.nuclphysbps.2006.09.101](https://doi.org/10.1016/j.nuclphysbps.2006.09.101), [hep-ph/0608307](https://arxiv.org/abs/hep-ph/0608307).
- [13] S. Moch, M. Rogal and A. Vogt, *Differences between charged-current coefficient functions*, Nucl. Phys. B **790**, 317 (2008), doi:[10.1016/j.nuclphysb.2007.09.022](https://doi.org/10.1016/j.nuclphysb.2007.09.022), [0708.3731](https://arxiv.org/abs/0708.3731).
- [14] J. Davies, A. Vogt, S. Moch and J. A. M. Vermaseren, *Non-singlet coefficient functions for charged-current deep-inelastic scattering to the third order in QCD*, PoS **DIS2016**, 059 (2016), doi:[10.22323/1.265.0059](https://doi.org/10.22323/1.265.0059), [1606.08907](https://arxiv.org/abs/1606.08907).
- [15] J. Blümlein, P. Marquard, C. Schneider and K. Schönwald, *The massless three-loop Wilson coefficients for the deep-inelastic structure functions F_2 , F_L , xF_3 and g_1* , JHEP **11**, 156 (2022), doi:[10.1007/JHEP11\(2022\)156](https://doi.org/10.1007/JHEP11(2022)156), [2208.14325](https://arxiv.org/abs/2208.14325).
- [16] S.-O. Moch, B. Ruijl, T. Ueda, J. A. M. Vermaseren and A. Vogt, *DIS coefficient functions at four loops in QCD and beyond*, PoS **LL2022**, 047 (2022), doi:[10.22323/1.416.0047](https://doi.org/10.22323/1.416.0047), [2208.11067](https://arxiv.org/abs/2208.11067).
- [17] S. Moch, J. A. M. Vermaseren and A. Vogt, *The Three loop splitting functions in QCD: The Nonsinglet case*, Nucl. Phys. B **688**, 101 (2004), doi:[10.1016/j.nuclphysb.2004.03.030](https://doi.org/10.1016/j.nuclphysb.2004.03.030), [hep-ph/0403192](https://arxiv.org/abs/hep-ph/0403192).
- [18] A. Vogt, S. Moch and J. A. M. Vermaseren, *The Three-loop splitting functions in QCD: The Singlet case*, Nucl. Phys. B **691**, 129 (2004), doi:[10.1016/j.nuclphysb.2004.04.024](https://doi.org/10.1016/j.nuclphysb.2004.04.024), [hep-ph/0404111](https://arxiv.org/abs/hep-ph/0404111).
- [19] T. van Ritbergen, J. A. M. Vermaseren and S. A. Larin, *The Four loop beta function in quantum chromodynamics*, Phys. Lett. B **400**, 379 (1997), doi:[10.1016/S0370-2693\(97\)00370-5](https://doi.org/10.1016/S0370-2693(97)00370-5), [hep-ph/9701390](https://arxiv.org/abs/hep-ph/9701390).
- [20] M. Czakon, *The Four-loop QCD beta-function and anomalous dimensions*, Nucl. Phys. B **710**, 485 (2005), doi:[10.1016/j.nuclphysb.2005.01.012](https://doi.org/10.1016/j.nuclphysb.2005.01.012), [hep-ph/0411261](https://arxiv.org/abs/hep-ph/0411261).

- [21] S. Moch, B. Ruijl, T. Ueda, J. A. M. Vermaseren and A. Vogt, *Low moments of the four-loop splitting functions in QCD*, Phys. Lett. B **825**, 136853 (2022), doi:[10.1016/j.physletb.2021.136853](https://doi.org/10.1016/j.physletb.2021.136853), [2111.15561](https://arxiv.org/abs/2111.15561).
- [22] G. Falcioni, F. Herzog, S. Moch and A. Vogt, *Four-loop splitting functions in QCD – The quark-quark case*, Phys. Lett. B **842**, 137944 (2023), doi:[10.1016/j.physletb.2023.137944](https://doi.org/10.1016/j.physletb.2023.137944), [2302.07593](https://arxiv.org/abs/2302.07593).
- [23] G. Falcioni, F. Herzog, S. Moch and A. Vogt, *Four-loop splitting functions in QCD – The gluon-to-quark case* (2023), [2307.04158](https://arxiv.org/abs/2307.04158).
- [24] T. Gehrmann, A. von Manteuffel, V. Sotnikov and T.-Z. Yang, *Complete N_f^2 contributions to four-loop pure-singlet splitting functions* (2023), [2308.07958](https://arxiv.org/abs/2308.07958).
- [25] G. Falcioni, F. Herzog, S. Moch, J. Vermaseren and A. Vogt, *The double fermionic contribution to the four-loop quark-to-gluon splitting function* (2023), [2310.01245](https://arxiv.org/abs/2310.01245).
- [26] S. Moch, B. Ruijl, T. Ueda, J. Vermaseren and A. Vogt, *Additional moments and x-space approximations of four-loop splitting functions in QCD* (2023), [2310.05744](https://arxiv.org/abs/2310.05744).
- [27] T. Gehrmann, A. von Manteuffel, V. Sotnikov and T.-Z. Yang, *The $N_f C_F^3$ contribution to the non-singlet splitting function at four-loop order* (2023), [2310.12240](https://arxiv.org/abs/2310.12240).
- [28] I. Bierenbaum, J. Blumlein and S. Klein, *Mellin Moments of the $O(\alpha_s^3)$ Heavy Flavor Contributions to unpolarized Deep-Inelastic Scattering at $Q^2 \gg m^2$ and Anomalous Dimensions*, Nucl. Phys. B **820**, 417 (2009), doi:[10.1016/j.nuclphysb.2009.06.005](https://doi.org/10.1016/j.nuclphysb.2009.06.005), [0904.3563](https://arxiv.org/abs/0904.3563).
- [29] H. Kawamura, N. A. Lo Presti, S. Moch and A. Vogt, *On the next-to-next-to-leading order QCD corrections to heavy-quark production in deep-inelastic scattering*, Nucl. Phys. B **864**, 399 (2012), doi:[10.1016/j.nuclphysb.2012.07.001](https://doi.org/10.1016/j.nuclphysb.2012.07.001), [1205.5727](https://arxiv.org/abs/1205.5727).
- [30] J. Ablinger, J. Blümlein, A. De Freitas, A. Hasselhuhn, A. von Manteuffel, M. Round, C. Schneider and F. Wißbrock, *The transition matrix element $a_{gq}(n)$ of the variable flavor number scheme at $\mathcal{O}(\alpha_s^3)$* , Nuclear Physics B **882**, 263 (2014), doi:<https://doi.org/10.1016/j.nuclphysb.2014.02.007>, [1402.0359](https://arxiv.org/abs/1402.0359).
- [31] J. Ablinger, A. Behring, J. Blümlein, A. De Freitas, A. Hasselhuhn, A. von Manteuffel, M. Round, C. Schneider and F. Wißbrock, *The 3-Loop Non-Singlet Heavy Flavor Contributions and Anomalous Dimensions for the Structure Function $F_2(x, Q^2)$ and Transversity*, Nucl. Phys. B **886**, 733 (2014), doi:[10.1016/j.nuclphysb.2014.07.010](https://doi.org/10.1016/j.nuclphysb.2014.07.010), [1406.4654](https://arxiv.org/abs/1406.4654).
- [32] J. Ablinger, A. Behring, J. Blümlein, A. De Freitas, A. von Manteuffel and C. Schneider, *The 3-loop pure singlet heavy flavor contributions to the structure function $F_2(x, Q^2)$ and the anomalous dimension*, Nucl. Phys. B **890**, 48 (2014), doi:[10.1016/j.nuclphysb.2014.10.008](https://doi.org/10.1016/j.nuclphysb.2014.10.008), [1409.1135](https://arxiv.org/abs/1409.1135).
- [33] J. Ablinger, A. Behring, J. Blümlein, A. De Freitas, A. Goedicke, A. von Manteuffel, C. Schneider and K. Schönwald, *The unpolarized and polarized single-mass three-loop heavy flavor operator matrix elements $A_{gg,Q}$ and $\Delta A_{gg,Q}$* , JHEP **12**, 134 (2022), doi:[10.1007/JHEP12\(2022\)134](https://doi.org/10.1007/JHEP12(2022)134), [2211.05462](https://arxiv.org/abs/2211.05462).
- [34] J. Ablinger, A. Behring, J. Blümlein, A. De Freitas, A. von Manteuffel, C. Schneider and K. Schönwald, *The first-order factorizable contributions to the three-loop massive operator matrix elements $A_{Qg}^{(3)}$ and $\Delta A_{Qg}^{(3)}$* (2023), [2311.00644](https://arxiv.org/abs/2311.00644).

- [35] J. Currie, T. Gehrmann, E. W. N. Glover, A. Huss, J. Niehues and A. Vogt, *N^3LO corrections to jet production in deep inelastic scattering using the Projection-to-Born method*, JHEP **05**, 209 (2018), doi:[10.1007/JHEP05\(2018\)209](https://doi.org/10.1007/JHEP05(2018)209), [1803.09973](https://arxiv.org/abs/1803.09973).
- [36] T. Gehrmann, A. Huss, J. Niehues, A. Vogt and D. M. Walker, *Jet production in charged-current deep-inelastic scattering to third order in QCD*, Phys. Lett. B **792**, 182 (2019), doi:[10.1016/j.physletb.2019.03.003](https://doi.org/10.1016/j.physletb.2019.03.003), [1812.06104](https://arxiv.org/abs/1812.06104).
- [37] M. Cacciari, F. A. Dreyer, A. Karlberg, G. P. Salam and G. Zanderighi, *Fully Differential Vector-Boson-Fusion Higgs Production at Next-to-Next-to-Leading Order*, Phys. Rev. Lett. **115**(8), 082002 (2015), doi:[10.1103/PhysRevLett.115.082002](https://doi.org/10.1103/PhysRevLett.115.082002), [Erratum: Phys.Rev.Lett. 120, 139901 (2018)], [1506.02660](https://arxiv.org/abs/1506.02660).
- [38] E. Mirkes and D. Zeppenfeld, *Dijet production at HERA in next-to-leading order*, Phys. Lett. B **380**, 205 (1996), doi:[10.1016/0370-2693\(96\)00426-1](https://doi.org/10.1016/0370-2693(96)00426-1), [hep-ph/9511448](https://arxiv.org/abs/hep-ph/9511448).
- [39] S. Catani and M. H. Seymour, *A General algorithm for calculating jet cross-sections in NLO QCD*, Nucl. Phys. B **485**, 291 (1997), doi:[10.1016/S0550-3213\(96\)00589-5](https://doi.org/10.1016/S0550-3213(96)00589-5), [Erratum: Nucl.Phys.B 510, 503–504 (1998)], [hep-ph/9605323](https://arxiv.org/abs/hep-ph/9605323).
- [40] D. Graudenz, *Disaster++: Version 1.0* (1997), [hep-ph/9710244](https://arxiv.org/abs/hep-ph/9710244).
- [41] Z. Nagy and Z. Trocsanyi, *Multijet cross-sections in deep inelastic scattering at next-to-leading order*, Phys. Rev. Lett. **87**, 082001 (2001), doi:[10.1103/PhysRevLett.87.082001](https://doi.org/10.1103/PhysRevLett.87.082001), [hep-ph/0104315](https://arxiv.org/abs/hep-ph/0104315).
- [42] V. Antonelli, M. Dasgupta and G. P. Salam, *Resummation of thrust distributions in DIS*, JHEP **02**, 001 (2000), doi:[10.1088/1126-6708/2000/02/001](https://doi.org/10.1088/1126-6708/2000/02/001), [hep-ph/9912488](https://arxiv.org/abs/hep-ph/9912488).
- [43] M. Dasgupta and G. P. Salam, *Resummed event shape variables in DIS*, JHEP **08**, 032 (2002), doi:[10.1088/1126-6708/2002/08/032](https://doi.org/10.1088/1126-6708/2002/08/032), [hep-ph/0208073](https://arxiv.org/abs/hep-ph/0208073).
- [44] I. Borsa, D. de Florian and I. Pedron, *Jet Production in Polarized Deep Inelastic Scattering at Next-to-Next-to-Leading Order*, Phys. Rev. Lett. **125**(8), 082001 (2020), doi:[10.1103/PhysRevLett.125.082001](https://doi.org/10.1103/PhysRevLett.125.082001), [2005.10705](https://arxiv.org/abs/2005.10705).
- [45] I. Borsa, D. de Florian and I. Pedron, *Inclusive-jet and dijet production in polarized deep inelastic scattering*, Phys. Rev. D **103**(1), 014008 (2021), doi:[10.1103/PhysRevD.103.014008](https://doi.org/10.1103/PhysRevD.103.014008), [2010.07354](https://arxiv.org/abs/2010.07354).
- [46] G. P. Salam and J. Rojo, *A Higher Order Perturbative Parton Evolution Toolkit (HOPPET)*, Comput. Phys. Commun. **180**, 120 (2009), doi:[10.1016/j.cpc.2008.08.010](https://doi.org/10.1016/j.cpc.2008.08.010), [0804.3755](https://arxiv.org/abs/0804.3755).
- [47] V. Bertone and A. Karlberg, *Benchmark of the deep-inelastic-scattering structure functions at $\mathcal{O}(\alpha_s^3)$* , CERN-TH-2024-018.
- [48] V. Bertone, S. Carrazza and J. Rojo, *APFEL: A PDF Evolution Library with QED corrections*, Comput. Phys. Commun. **185**, 1647 (2014), doi:[10.1016/j.cpc.2014.03.007](https://doi.org/10.1016/j.cpc.2014.03.007), [1310.1394](https://arxiv.org/abs/1310.1394).
- [49] V. Bertone, *APFEL++: A new PDF evolution library in C++*, PoS DIS2017, 201 (2018), doi:[10.22323/1.297.0201](https://doi.org/10.22323/1.297.0201), [1708.00911](https://arxiv.org/abs/1708.00911).
- [50] F. A. Dreyer and A. Karlberg, *Vector-Boson Fusion Higgs Production at Three Loops in QCD*, Phys. Rev. Lett. **117**(7), 072001 (2016), doi:[10.1103/PhysRevLett.117.072001](https://doi.org/10.1103/PhysRevLett.117.072001), [1606.00840](https://arxiv.org/abs/1606.00840).

- [51] F. A. Dreyer and A. Karlberg, *Vector-Boson Fusion Higgs Pair Production at N^3LO* , Phys. Rev. D **98**(11), 114016 (2018), doi:[10.1103/PhysRevD.98.114016](https://doi.org/10.1103/PhysRevD.98.114016), [1811.07906](https://arxiv.org/abs/1811.07906).
- [52] F. A. Dreyer and A. Karlberg, *Fully differential Vector-Boson Fusion Higgs Pair Production at Next-to-Next-to-Leading Order*, Phys. Rev. D **99**(7), 074028 (2019), doi:[10.1103/PhysRevD.99.074028](https://doi.org/10.1103/PhysRevD.99.074028), [1811.07918](https://arxiv.org/abs/1811.07918).
- [53] A. Karlberg, P. Nason, G. Salam, G. Zanderighi and F. Dreyer, *Hoppet v1.3.0 release note*, CERN-TH-2023-237, MPP-2023-285, OUTP-23-15P.
- [54] M. Cacciari, G. P. Salam and G. Soyez, *FastJet User Manual*, Eur. Phys. J. C **72**, 1896 (2012), doi:[10.1140/epjc/s10052-012-1896-2](https://doi.org/10.1140/epjc/s10052-012-1896-2), [1111.6097](https://arxiv.org/abs/1111.6097).
- [55] A. Buckley, J. Ferrando, S. Lloyd, K. Nordström, B. Page, M. Rüfenacht, M. Schönherr and G. Watt, *LHAPDF6: parton density access in the LHC precision era*, Eur. Phys. J. C **75**, 132 (2015), doi:[10.1140/epjc/s10052-015-3318-8](https://doi.org/10.1140/epjc/s10052-015-3318-8), [1412.7420](https://arxiv.org/abs/1412.7420).
- [56] S. Alioli, P. Nason, C. Oleari and E. Re, *A general framework for implementing NLO calculations in shower Monte Carlo programs: the POWHEG BOX*, JHEP **06**, 043 (2010), doi:[10.1007/JHEP06\(2010\)043](https://doi.org/10.1007/JHEP06(2010)043), [1002.2581](https://arxiv.org/abs/1002.2581).
- [57] I. Borsa, D. de Florian and I. Pedron, *Dijet production in neutral current and charged current polarized deep inelastic scattering*, Phys. Rev. D **105**(7), 074025 (2022), doi:[10.1103/PhysRevD.105.074025](https://doi.org/10.1103/PhysRevD.105.074025), [2112.08223](https://arxiv.org/abs/2112.08223).
- [58] I. Borsa, D. de Florian and I. Pedron, *The full set of polarized deep inelastic scattering structure functions at NNLO accuracy*, Eur. Phys. J. C **82**(12), 1167 (2022), doi:[10.1140/epjc/s10052-022-11140-z](https://doi.org/10.1140/epjc/s10052-022-11140-z), [2210.12014](https://arxiv.org/abs/2210.12014).
- [59] I. Borsa, D. de Florian and I. Pedron, *NNLO jet production in neutral and charged current polarized deep inelastic scattering*, Phys. Rev. D **107**(5), 054027 (2023), doi:[10.1103/PhysRevD.107.054027](https://doi.org/10.1103/PhysRevD.107.054027), [2212.06625](https://arxiv.org/abs/2212.06625).
- [60] R. Abdul Khalek et al., *Snowmass 2021 White Paper: Electron Ion Collider for High Energy Physics* (2022), [2203.13199](https://arxiv.org/abs/2203.13199).
- [61] R. Devenish and A. Cooper-Sarkar, *Deep inelastic scattering*, doi:[10.1093/acprof:oso/9780198506713.001.0001](https://doi.org/10.1093/acprof:oso/9780198506713.001.0001) (2004).
- [62] F. D. Aaron et al., *Inclusive Deep Inelastic Scattering at High Q^2 with Longitudinally Polarised Lepton Beams at HERA*, JHEP **09**, 061 (2012), doi:[10.1007/JHEP09\(2012\)061](https://doi.org/10.1007/JHEP09(2012)061), [1206.7007](https://arxiv.org/abs/1206.7007).
- [63] G. P. Lepage, *A New Algorithm for Adaptive Multidimensional Integration*, J. Comput. Phys. **27**, 192 (1978), doi:[10.1016/0021-9991\(78\)90004-9](https://doi.org/10.1016/0021-9991(78)90004-9).
- [64] G. Watt, *Parton distribution function dependence of benchmark Standard Model total cross sections at the 7 TeV LHC*, JHEP **09**, 069 (2011), doi:[10.1007/JHEP09\(2011\)069](https://doi.org/10.1007/JHEP09(2011)069), [1106.5788](https://arxiv.org/abs/1106.5788).
- [65] S. Bailey, T. Cridge, L. A. Harland-Lang, A. D. Martin and R. S. Thorne, *Parton distributions from LHC, HERA, Tevatron and fixed target data: MSHT20 PDFs*, Eur. Phys. J. C **81**(4), 341 (2021), doi:[10.1140/epjc/s10052-021-09057-0](https://doi.org/10.1140/epjc/s10052-021-09057-0), [2012.04684](https://arxiv.org/abs/2012.04684).

- [66] J. McGowan, T. Cridge, L. A. Harland-Lang and R. S. Thorne, *Approximate N^3LO parton distribution functions with theoretical uncertainties: MSHT20a N^3LO PDFs*, Eur. Phys. J. C **83**(3), 185 (2023), doi:[10.1140/epjc/s10052-023-11236-0](https://doi.org/10.1140/epjc/s10052-023-11236-0), [Erratum: Eur.Phys.J.C 83, 302 (2023)], [2207.04739](https://arxiv.org/abs/2207.04739).
- [67] M. Cacciari, G. P. Salam and G. Soyez, *The anti- k_t jet clustering algorithm*, JHEP **04**, 063 (2008), doi:[10.1088/1126-6708/2008/04/063](https://doi.org/10.1088/1126-6708/2008/04/063), [0802.1189](https://arxiv.org/abs/0802.1189).
- [68] J. L. Feng, I. Galon, F. Kling and S. Trojanowski, *ForwArd Search ExpeRiment at the LHC*, Phys. Rev. D **97**(3), 035001 (2018), doi:[10.1103/PhysRevD.97.035001](https://doi.org/10.1103/PhysRevD.97.035001), [1708.09389](https://arxiv.org/abs/1708.09389).
- [69] T. Gottschalk, *Chromodynamic Corrections to Neutrino Production of Heavy Quarks*, Phys. Rev. D **23**, 56 (1981), doi:[10.1103/PhysRevD.23.56](https://doi.org/10.1103/PhysRevD.23.56).
- [70] E. Laenen, S. Riemersma, J. Smith and W. L. van Neerven, *Complete $O(\alpha_s)$ corrections to heavy flavor structure functions in electroproduction*, Nucl. Phys. B **392**, 162 (1993), doi:[10.1016/0550-3213\(93\)90201-Y](https://doi.org/10.1016/0550-3213(93)90201-Y).
- [71] E. Laenen, S. Riemersma, J. Smith and W. L. van Neerven, *$O(\alpha_s)$ corrections to heavy flavor inclusive distributions in electroproduction*, Nucl. Phys. B **392**, 229 (1993), doi:[10.1016/0550-3213\(93\)90202-Z](https://doi.org/10.1016/0550-3213(93)90202-Z).
- [72] M. Gluck, S. Kretzer and E. Reya, *Detailed next-to-leading order analysis of deep inelastic neutrino induced charm production off strange sea partons*, Phys. Lett. B **398**, 381 (1997), doi:[10.1016/S0370-2693\(97\)00232-3](https://doi.org/10.1016/S0370-2693(97)00232-3), [Erratum: Phys.Lett.B 405, 392 (1997)], [hep-ph/9701364](https://arxiv.org/abs/hep-ph/9701364).
- [73] J. Blumlein, A. Hasselhuhn, P. Kovacikova and S. Moch, *$O(\alpha_s)$ Heavy Flavor Corrections to Charged Current Deep-Inelastic Scattering in Mellin Space*, Phys. Lett. B **700**, 294 (2011), doi:[10.1016/j.physletb.2011.05.007](https://doi.org/10.1016/j.physletb.2011.05.007), [1104.3449](https://arxiv.org/abs/1104.3449).
- [74] A. Behring, J. Blümlein, A. De Freitas, A. Hasselhuhn, A. von Manteuffel and C. Schneider, *$O(\alpha_s^3)$ heavy flavor contributions to the charged current structure function $xF_3(x, Q^2)$ at large momentum transfer*, Phys. Rev. D **92**(11), 114005 (2015), doi:[10.1103/PhysRevD.92.114005](https://doi.org/10.1103/PhysRevD.92.114005), [1508.01449](https://arxiv.org/abs/1508.01449).
- [75] E. L. Berger, J. Gao, C. S. Li, Z. L. Liu and H. X. Zhu, *Charm-Quark Production in Deep-Inelastic Neutrino Scattering at Next-to-Next-to-Leading Order in QCD*, Phys. Rev. Lett. **116**(21), 212002 (2016), doi:[10.1103/PhysRevLett.116.212002](https://doi.org/10.1103/PhysRevLett.116.212002), [1601.05430](https://arxiv.org/abs/1601.05430).
- [76] J. Gao, *Massive charged-current coefficient functions in deep-inelastic scattering at NNLO and impact on strange-quark distributions*, JHEP **02**, 026 (2018), doi:[10.1007/JHEP02\(2018\)026](https://doi.org/10.1007/JHEP02(2018)026), [1710.04258](https://arxiv.org/abs/1710.04258).
- [77] A. Banfi, S. F. Ravasio, B. Jäger, A. Karlberg, F. Reichenbach and G. Zanderighi, *A POWHEG generator for deep inelastic scattering* (2023), [2309.02127](https://arxiv.org/abs/2309.02127).